Cell

A Nutrient-Responsive Pathway that Determines M Phase Timing through Control of B-Cyclin mRNA Stability

Vincent Messier,[1] Daniel Zenklusen,[1] and Stephen W. Michnick[1,*]
[1]Département de Biochimie, Université de Montréal, C.P. 6128, Succursale centre-ville, Montréal, Québec H3C 3J7, Canada
*Correspondence: stephen.michnick@umontreal.ca
http://dx.doi.org/10.1016/j.cell.2013.04.035

SUMMARY

The rate of cell-cycle progression must be tuned in response to nutrient levels to ensure that sufficient materials are synthesized to generate viable daughters. We report that accumulation of the yeast M phase B-cyclin *CLB2* mRNA depends on assembly and activation of the heterogeneous nuclear RNA-binding protein (hnRNP) arginine methyltransferase Hmt1, which is promoted by the kinase Dbf2 and countered by the PP2A phosphatase Pph22. Activated Hmt1 methylates hnRNPs, which in turn stabilize *CLB2* transcripts. Dbf2 activation of Hmt1 is highly cooperative, producing a sharp increase in *CLB2*, whereas Pph22 dephosphorylation is graded such that small changes in PP2A activity can cause large shifts in Dbf2-mediated Hmt1 activity. Starvation and rapamycin inhibition of TOR activate Pph22, causing a depletion of *CLB2* and delay of M phase. We propose a general model wherein changes to Pph22 activity modulate cyclin mRNA stability to tune cell-cycle progression to environmental conditions.

INTRODUCTION

Transcriptional programs and thus messenger RNA (mRNA) expression patterns constantly adapt to cell-cycle control mechanisms. We have little understanding, however, of how posttranscriptional mRNA regulation contributes to the control of mitosis (Romero-Santacreu et al., 2009). mRNA decay is modulated by proteins that bind untranslated regions (UTRs) or open reading frames (ORFs) of mRNA, thereby inducing or preventing their decay. Most mRNA decay machinery is located in the cytosol (reviewed in Houseley and Tollervey, 2009). Early factors, such as the heterogeneous nuclear RNA-binding proteins (hnRNPs), bind cotranscriptionally to mRNA upon posttranslational arginine methylation to promote mRNA export and stability (Yu et al., 2004). How mRNA regulation is linked to cell-cycle and signal-transduction machinery remains the subject of intense investigation.

Recently, a mechanism that controls decay of M phase cyclin *CLB2* mRNA was reported in the budding yeast *S. cerevisiae* (Trcek et al., 2011). *CLB2* mRNA levels increase early in and then are rapidly degraded at the end of M phase. Trcek et al. demonstrated that *CLB2* transcript decay is regulated by promoter-dependent cotranscriptional recruitment of the mitotic exit-regulating kinase Dbf2. Other proteins, including hnRNPs, are recruited to the *CLB2* locus to promote mRNA stability and nuclear export. No specific links, however, have been made between recruitment of these proteins and Dbf2 activity (Yu et al., 2004).

There is some evidence that starvation-mediated cell-cycle delays may be regulated through control of RNA stability. Starvation is interpreted in part by the TOR pathway, and rapamycin-induced TOR inhibition mimics the starvation response. G1 cell-cycle progression is affected by both nitrogen starvation and rapamycin through reduction of G1 cyclin transcription and translation (Barbet et al., 1996). Rapamycin also delays or arrests different cell-cycle phases, but mechanisms underlying these responses are unknown (Nakashima et al., 2008). Rapamycin prevents TOR phosphorylation of the substrates protein S6 kinase and initiation factor (eIF) 4E binding protein 1, resulting in downregulation of translation and accompanying pleotropic effects (Chung et al., 1992). Interestingly though, the TOR pathway delays early M phase progression in a translation-independent manner (Nakashima et al., 2008). Based on these observations and those of Trcek et al., we hypothesized that a TOR-regulated pathway may control M phase cyclin stability posttranscriptionally, via mechanisms that regulate mRNA decay (Trcek et al., 2011).

We have discovered a pathway that links starvation to control of *CLB2* mRNA stability and M phase delay. Dbf2 phosphorylates and activates the arginine methyltransferase Hmt1. In turn, Hmt1 methylates hnRNPs, promoting their nuclear localization, their cotranscriptional association with *CLB2* mRNA, and the stability of *CLB2* mRNA. Rapamycin inhibition of TOR or starvation induces recruitment of the PP2A phosphatase Pph22 to Hmt1, dephosphorylation of Hmt1, and simultaneous dissociation of Dbf2 from Hmt1. Hmt1 is inactivated, preventing methylation of hnRNPs and thus failure of *CLB2* mRNA to accumulate in M phase.

RESULTS

Rapamycin Delays Early M Phase

Delayed early M phase was reported for rapamycin treatment and nutrient starvation (Nakashima et al., 2008). To confirm these

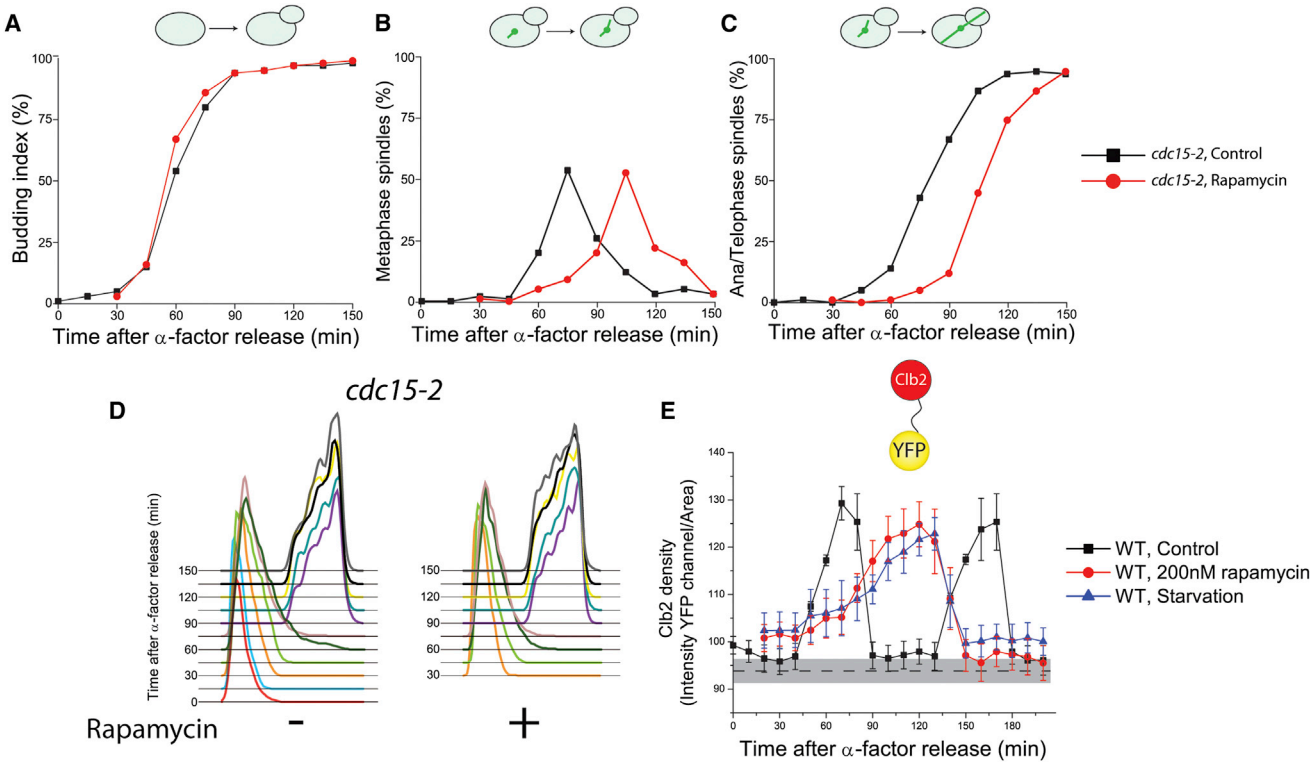

Figure 1. Delays in early M Phase in Rapamycin-Treated and Starved Cells Correlate with Slow Clb2 Accumulations

(A–D) Synchronized *cdc15-2* temperature-sensitive mutant strains grown at restrictive temperatures were fixed, and the budded cell proportions (A), metaphase (B), and anaphase/telophase spindle proportions (C) and DNA content stained with PI (D) measured by microscopy and FACS analysis.

(E) Fluorescent protein-tagged Clb2 quantification was performed for 100 cells in rapamycin and starvation.

Error bars, standard deviation (SD) (n = 100).

conclusions, we monitored (1) bud emergence (Figure 1A), (2) bipolar metaphase spindle emergence and anaphase/telophase spindle entry into the bud by Tub1 immunostaining (Figures 1B and 1C) (St-Pierre et al., 2009), and (3) DNA synthesis by propidium iodide (PI) staining and fluorescence-activated cell sorting (FACS) detection (Figure 1D). Experiments were performed with α factor-synchronized *cdc15-2* mutant strain at restrictive temperature (i.e., limiting the cell cycle to between G1 and telophase) and treated with or without 200 nM rapamycin. Early M phase transition was delayed by 30 min in rapamycin, as indicated by a delay in metaphase spindle emergence compared to control cells. In contrast, maximal PI DNA staining was observed after 90 min, in both conditions, confirming that rapamycin exclusively causes early M phase delay, not delay in S phase exit.

Rapamycin and Starvation Delay Clb2 Protein Synthesis

We used endogenous cyclin B, Clb2-yellow fluorescent protein (YFP) fusion to measure protein abundance. Cells were synchronized with α factor, treated with 200 nM rapamycin or control, or placed in starvation medium, identical to the medium used by Nakashima et al. (Table S1 available online). Twenty minutes after α factor release, Clb2-YFP fluorescence was imaged every 10 min for 200 min. We quantified YFP intensities normalized to cell area for each of 100 cells (Figure 1E). Clb2 synthesis peaked at 70 and 160 min. In rapamycin or starved cells, however, Clb2 increased slowly, reaching peak intensity at 120 min, consistent with the previously reported M phase delay in both rapamycin-treated and starved cells (Nakashima et al., 2008).

CLB2 mRNA Fails to Accumulate in M Phase in Rapamycin-Treated or Starved Cells

We next determined whether changes in Clb2 protein accumulation were due to transcriptional or posttranscriptional regulation of *CLB2* mRNA. To achieve this, we performed single-molecule fluorescence in situ hybridization (FISH) to detect individual *CLB2* and control *ACT1* mRNAs in single cells (Trcek et al., 2011; Zenklusen et al., 2008) (Figure 2A). We also measured nuclear-localized transcriptional foci to estimate nascent mRNA numbers, which are affected by initiation rate and postinitiation, elongation, and termination times for production of immature mRNA (Trcek et al., 2011). Cells were synchronized, incubated with rapamycin or in starvation medium 20 min after α factor release, and fixed every 15 min, and nascent (Figure 2B) and cytoplasmic mRNA were counted (Figure 2C). Control cells accumulated up to three nascent *CLB2* mRNA molecules in M phase. In starved or rapamycin-treated cells, *CLB2* nascent transcript stayed at this maximum for an additional 60 min, consistent with prolonged transcription of *CLB2* due to delayed cell-cycle progression. However, cytosolic *CLB2*

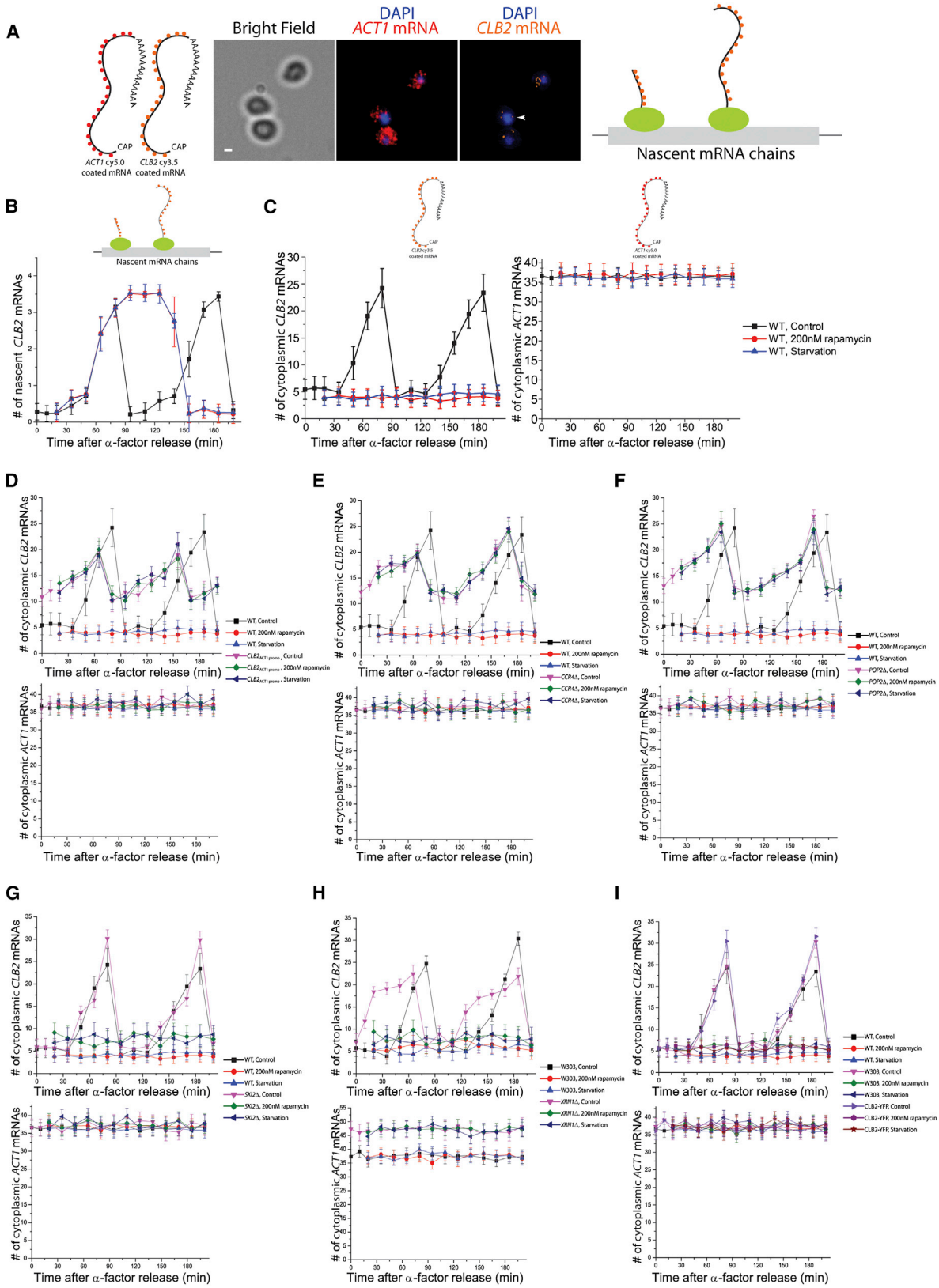

(legend on next page)

mRNA remained at basal levels in rapamycin-treated or starved cells, suggesting posttranscriptional regulation of *CLB2* mRNA.

CLB2 Decay Is Mediated by CCR4-NOT and XRN1 Exoribonuclease Activities

Trcek et al. reported that *CLB2* mRNA decay is primed with *CLB2* promoter-associated proteins and suggested that regulated mRNA decay implicates the CCR4-NOT complex (Trcek et al., 2011). Consistent with this hypothesis, we found that expression of *CLB2* transcripts under the *ACT1* promoter resulted in unregulated accumulation under all conditions with the exception of the typical drop in copy number following cell division (Figure 2D) (Gandhi et al., 2011). *ACT1* message number itself does not drop following cell division, typical of what has been observed in previous studies (Pramila et al., 2006). Moreover, cytoplasmic accumulation is restored in cells lacking *CCR4* and *POP2*, two components of the CCR4-NOT complex, revealing a direct role of CCR4-NOT in the regulated decay of *CLB2* mRNA. *CLB2* mRNA degradation following CCR4-NOT-mediated deadenylation may be redundant and achieved by either 5′ to 3′ or 3′ to 5′ degradation, as mutations in either of the two pathways only marginally affect wild-type (WT) *CLB2* mRNA levels (Figures 2E–2H). Furthermore, increases in *CLB2* transcripts were identical in both WT strains and those expressing the Clb2-YFP fusion (Figure 2I). Finally, *CLB2* mRNA turnover in nutrient-starved and rapamycin-treated cells was specific, since *ACT1* transcripts remained constant, with the exception of the *XRN1* mutant.

Rapamycin Causes Sequestering of hnRNPs in the Nucleus

hnRNP deletions result in decay of cytosolic mRNA or its accumulation in the nucleus (Hector et al., 2002; Kerr et al., 2011). We thus tested whether rapamycin could induce similar results. We used diploid strains that express one of each of the endogenous hnRNPs Nab2, Npl3, and Hrp1 as green fluorescent protein (GFP) fusions and endogenous Nup49-dtTomato fusion as a nuclear membrane marker. Strains were treated with rapamycin for 6 hr and imaged (Figure 3A). We quantified GFP signal intensities over the nucleus, the cytoplasm, and the whole cell and normalized the quantity by area for 100 cells (Figure 3B). hnRNP-GFP signals remained unaffected in the nucleus, but we observed a significant decrease of cytoplasm fluorescence to autofluorescent levels. This rapamycin-induced nuclear sequestration was specific to the hnRNPs Nab2, Npl3, and Hrp1; no effects were observed on mRNA export receptor Mex67 or karyopherins (Figures S1A and S1B). Importantly, an Npl3 mutant that cannot be arginine methylated did not stabilize *CLB2* transcripts. Together these data suggest a direct link between hnRNP methylation, localization, and *CLB2* mRNA decay (Figure 3C) (McBride et al., 2005).

Hmt1 Arginine Methyltransferase Activity Is Abolished in Rapamycin-Treated Cells

As Hmt1 is the likely candidate for hnRNP arginine methyltransferase, we tested whether Hmt1 purified from rapamycin-treated cells could methylate hnRNPs in vitro. We performed a methylation assay on TAP-tagged purified yeast Nab2 and Npl3 with radiolabeled methyl donor S-adenosyl-L-[methyl-^{3}H]-methionine (^{3}H-SAM) incubated with purified Hmt1-TAP from strains treated or not treated with rapamycin for 6 hr. We used western blotting of the methylation reactions with anti-TAP tag CBP antibody to verify protein expression and stability of each TAP fusion (Figure S1C). Both Nab2 and Npl3 were Hmt1 substrates in vitro, but Hmt1 from rapamycin-treated strains did not methylate these proteins.

Rapamycin Does Not Affect Hmt1 Activity through Changes in Its Expression or Localization

We used a yeast strain expressing endogenous Hmt1-GFP and treated or did not treat cells with rapamycin for 6 hr. Hmt1 expression was quantified by FACS (Figure S2A). Surprisingly, rapamycin-treated cells showed 10-fold increase in Hmt1 expression in the nucleus and cytosol (Figures S2B and S2C). Thus, rapamycin likely causes a loss in Hmt1 activity, not expression.

Rapamycin Prevents Hmt1 Homo-oligomerization and Activation

Hmt1 is only active as dimers to hexamers (Weiss et al., 2000). We tested whether rapamycin prevents Hmt1 oligomerization. We devised a simple in vivo assay to detect oligomeric states of Hmt1 based on affinity and immunoaffinity detection of dual-immunogenic peptide-tagged Hmt1 (Figure 4A). We generated a diploid reporter strain in which a TAP tag is introduced at one Hmt1 locus and an antigenic mouse dihydrofolate reductase (DFHR F[3]) is introduced at the second locus. Following rapamycin treatment, we performed Hmt1-TAP immunoglobulin G (IgG) immunoprecipitation (IP) (with antibody against TAP tag protein A domain) and eluted and ran samples on SDS-PAGE followed by immunoblot with an antibody against either DHFR F[3] or the TAP CBP domain (Figure 4B). Under rapamycin treatment, Hmt1-TAP prevented Hmt1-DHFR F[3] coIP, suggesting that rapamycin prevents Hmt1 oligomerization and activation.

Figure 2. *CLB2* mRNA Fails to Accumulate in Early M Phase in Rapamycin-Treated and Starved Cells

(A) cy3.5 *CLB2* (in orange) and cy5.0 *ACT1* (in red) mRNA probes were combined to reveal single-cell, single-molecule mRNAs by FISH and to detect mRNA accumulation. Cell nuclei were stained with DAPI (in blue). Nascent mRNA chains were estimated from transcriptional foci delimited in the nucleus (arrowhead).

(B) Fluorescent *CLB2* nascent mRNA counting was performed for 50 cells in rapamycin-treated or starved cells. Error bars, SD (n = 50).

(C) Fluorescent *CLB2* (left panel) and *ACT1* (right panel) mRNA counting was performed for 50 cells in rapamycin-treated or starved cells. Error bars, SD (n = 50).

(D–I) Expression of *CLB2* from ACT1 promoter (D), *CCR4*Δ (E), *POP2*Δ (F), *XRN1*Δ (G), and *SKI2*Δ (H) knockout strains, and W303 and CLB2-YFP (I) strains was synchronized, and mRNA accumulation was detected with a mixture of cy3.5 *CLB2* and cy5.0 *ACT1* mRNA probes to reveal single-cell, single-molecule mRNAs by FISH. Cytoplasmic *CLB2* (upper panels) and *ACT1* (lower panels) mRNA counting was performed for 50 cells in rapamycin-treated or starved cells. Error bars, SD (n = 50). Scale bar: 1 μm.

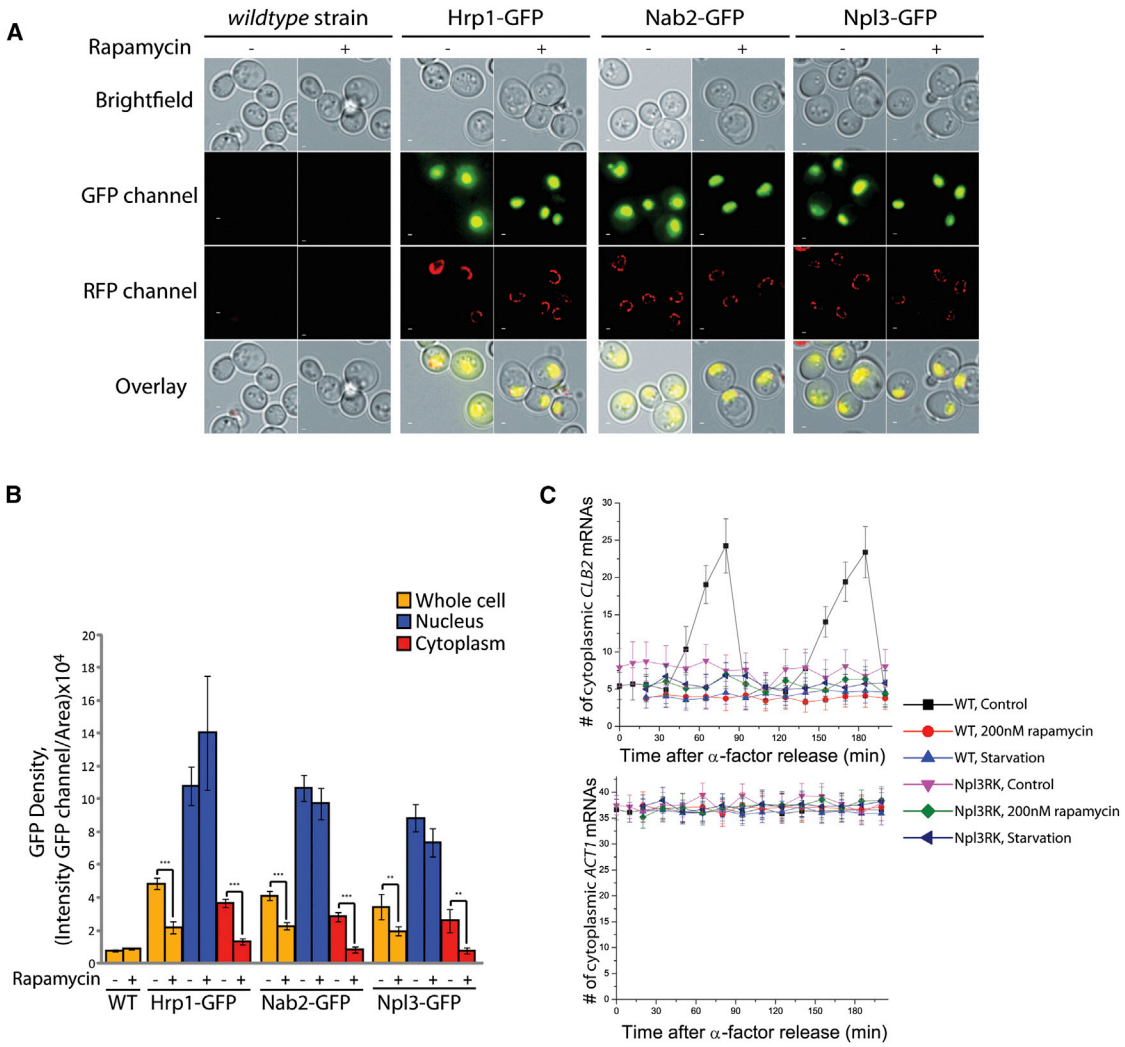

Figure 3. hnRNPs Are Sequestered in the Nuclei of Rapamycin-Treated Cells

(A) hnRNPs fused to GFP-expressing strains (in green) and Nup49 fused to dtTomato-expressing strains (in red; as nuclear membrane marker) were treated with rapamycin for 6 hr. Cells were imaged and overlaid.

(B) GFP intensities for hnRNPs fused to GFP were quantified and area normalized for 100 cells in rapamycin (in yellow). Segmented GFP signal into nucleus (in blue) and cytoplasm (in red) is based on nuclear membrane marker. Error bars, SD (n = 100).

(C) Npl3RK mutant strain was synchronized, and mRNA accumulation detected with a mixture of cy3.5 *CLB2* and cy5.0 *ACT1* mRNA probes to reveal single-cell, single-molecule mRNAs by FISH. Cytoplasmic *CLB2* (upper panel) and *ACT1* (lower panel) mRNA counting was performed for 50 cells in rapamycin-treated or starved cells. Error bars, SD (n = 50). Scale bar: 1 μm.

See also Figure S1.

Hmt1 Oligomerization and Activity Are Ser9 Phosphorylation Dependent

We observed that a fraction of Hmt1 migrated slowly on SDS-PAGE in the control cells (Hmt1*); this is not observed under rapamycin treatment (Figure 4B). Hmt1* disappeared within 10 min after rapamycin treatment, which corresponds to the time when Hmt1 oligomer dissociation reaches a steady state as measured in vivo with the *R. reniformis* luciferase (Rluc) reporter PCA (Malleshaiah et al., 2010) (Figures 4C and 4D). We reasoned that this species could be phosphorylated, and phosphorylation could be required for oligomerization, and thus, we set out to identify potential sites of phosphorylation. A clue was provided by the crystal structure (Weiss et al., 2000). Hmt1 was crystallized as an active hexamer. However, the form of Hmt1 used was an N-terminal truncation of 20 amino acids (Weiss et al., 2000). We hypothesized that these residues could contain phosphorylation sites involved in oligomerization. If these sites are necessary for Hmt1 oligomerization, they should be conserved. We aligned Hmt1 homolog sequences for *ascomycetes* fungi (Figure S2D) (Lord et al., 2002). Five potential sites were conserved, of which Ser9 and Tyr23 were the most likely phosphorylate candidates (NetPhos 2.0) (Blom et al., 1999) (Figure S2E).

We investigated whether Hmt1 hexamerization depends on Ser9 phosphorylation. We adapted the TAP tag IP assay

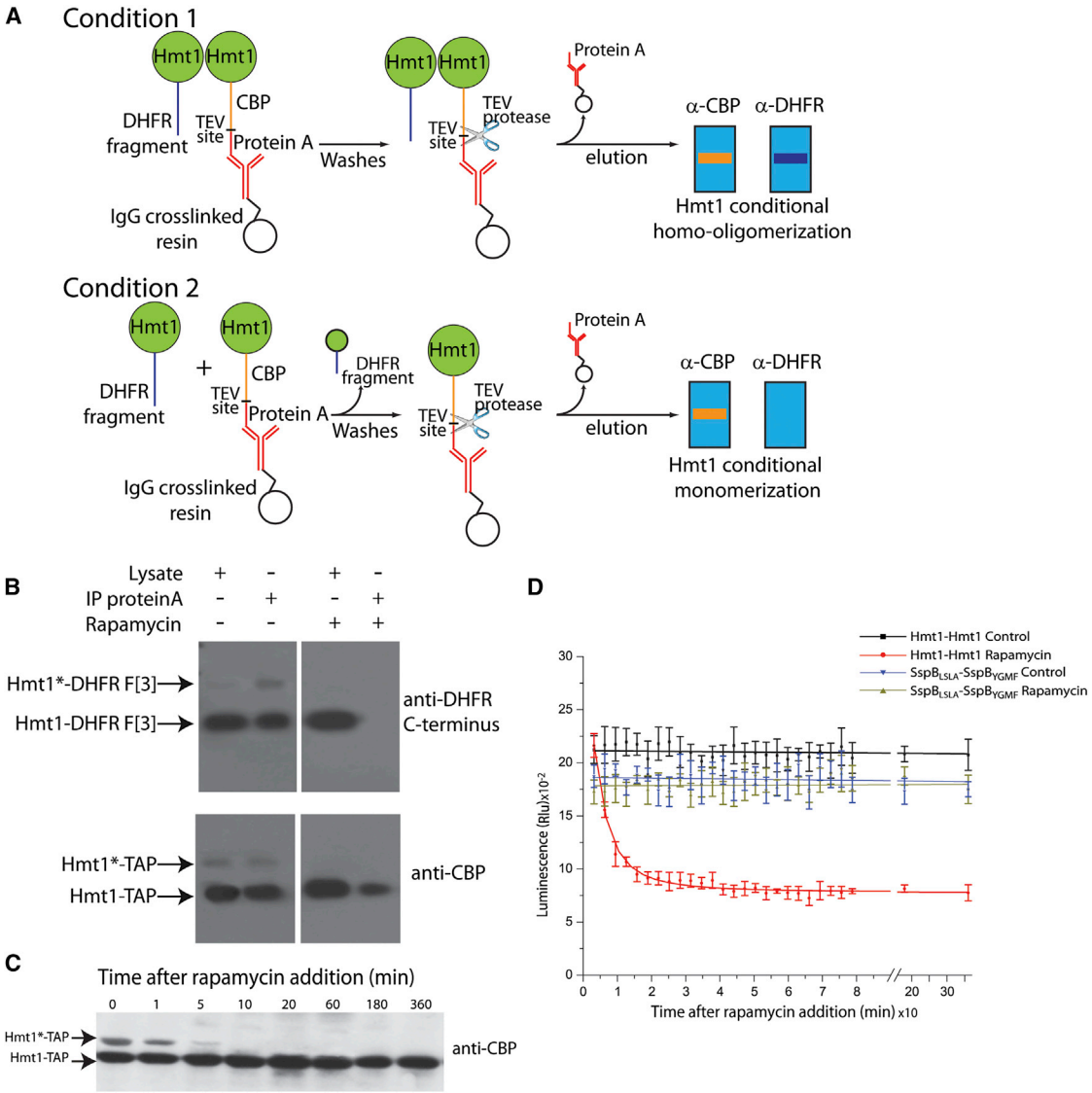

Figure 4. Both Hmt1 Low-Mobility Species and Homo-oligomers Are Lost in Rapamycin-Treated Cells

(A) Flow chart of modified TAP tag purification for Hmt1 complexes.

(B) TAP tag purification for Hmt1 complexes was performed for cells treated with rapamycin for 6 hr. For each condition, Hmt1 coIP complex and cell lysates were analyzed by immunoblotting.

(C) TAP tag purification for Hmt1 fusion proteins by IgG IPs was analyzed by anti-CBP immunoblotting after rapamycin treatments (200 nM).

(D) Time course in vivo dynamic analysis of Hmt1 oligomerization reported by Rluc PCA as a function of time after rapamycin (200 nM) addition to media. PPIs reported by Rluc PCA were tested for positive control SspB$_{LSLA}$-SspB$_{YGMF}$ interaction.

Error bars, standard error of the mean (SEM) (n = 3). See also Figure S2.

(Figure 5A) to include a step to deplete phosphorylated species with alkaline phosphatase (AP) following Hmt1-TAP IP. Protein was applied on IgG resin with AP or vanadate-inactivated AP for 1 hr (Figure 5B). In vanadate-inactivated AP samples, Hmt1-TAP IPs copurified with Hmt1-DHFR F[3] but not in samples with active AP. These results suggest that Hmt1 hexamer requires phosphorylation of Ser9.

To determine whether Ser9 phosphorylation is required and sufficient for Hmt1 hexamer, we generated phosphomimetic (Hmt1S9E) and nonphosphorylatable (Hmt1S9A) mutants. We generated Hmt1 homo-oligomer reporter strains as above for WT Hmt1 (Hmt1WT-TAP), Hmt1S9E, or Hmt1S9A and performed our IP assay (Figure 5B). Notably, the Hmt1* species disappeared from anti-CBP blots of Hmt1S9E-TAP and Hmt1S9E-TAP, suggesting that Hmt1* does indeed represent a phosphorylated form of Hmt1 (Figure 5B). Furthermore, we observed that under AP treatment, Hmt1S9E-TAP copurified with Hmt1WT-DHFR F[3], which shows that Ser9 phosphomimetic mutation is sufficient to hexamerize Hmt1 with dephosphorylated Hmt1.

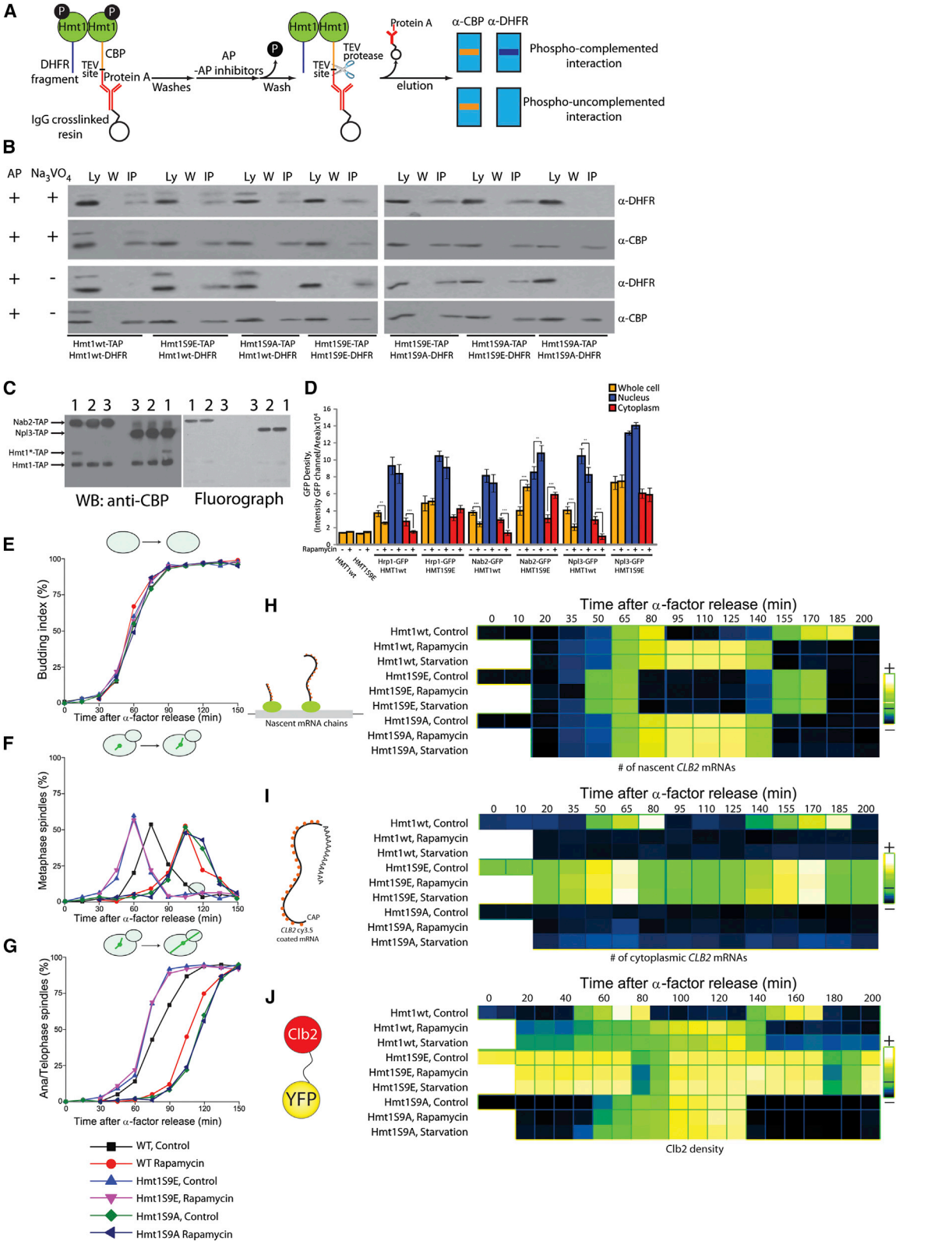

(legend on next page)

In contrast, AP-treated Hmt1S9A-TAP IPs no longer interacted with Hmt1WT-DHFR F[3], but, interestingly, both Hmt1WT-DHFR F[3] forms (Hmt1 and Hmt1*) copurified in vanadate-AP-treated Hmt1S9A-TAP IP. Thus the composition of the IPs is possibly equal parts Hmt1S9A/Hmt1/Hmt1*, or in other words, only one in three species need to be phosphorylated to create Hmt1 oligomers.

We were able to copurify any combination of Hmt1S9A and Hmt1S9E fused to DHFR F[3] or TAP under AP, with the exception of Hmt1S9A-TAP IPs failing to copurify Hmt1S9A-DHFR F[3] under both active and inactive AP treatments, suggesting that Hmt1 hexamer assembly must begin with a Hmt1*-Hmt1 dimeric complex.

Finally, we performed the methylation assay described above with purified Hmt1S9E-TAP or Hmt1S9A-TAP (Figure 5C). Both purified Nab2 and Npl3 were Hmt1S9E substrates in vitro. However, Hmt1S9A did not methylate these substrates.

hnRNP Nuclear Export Depends on Hmt1 Phosphorylation

Because Hmt1 methylation promotes hnRNP nuclear export, we investigated whether Hmt1S9E expression prevents rapamycin-induced hnRNP nuclear sequestration. We generated strains harboring an expression vector for WT *HMT1* (Hmt1WT) or HMT1S9E and simultaneously expressed one of each hnRNP (Nab2, Npl3, and Hrp1) fused to GFP and Nup49-dtTomato as nuclear membrane marker; strains were imaged and analyzed as described above (Figure S3A). In rapamycin-treated Hmt1WT cells, GFP signals for all three hnRNPs were sequestered in the nucleus, but Hmt1S9E cells showed significant cytoplasmic signal (Figure 5D). Distributions of other karyopherins were not affected (Figure S3B).

Hmt1 Phosphorylation State Determines M Phase Timing

We next tested whether Hmt1 activity affects the timing of the G2-M transition. We analyzed our cell-cycle markers, as described above for WT, in Hmt1 mutant strains and scored onset of budding (Figure 5E), DNA content (Figure S3D), and metaphase-to-telophase spindle formation (Figures 5F and 5G) (St-Pierre et al., 2009). We integrated HMT1S9E and HMT1S9A mutations directly into the HMT1 genomic locus in the *cdc15-2* strain. We observed an accelerated M phase transition in the Hmt1S9E strain, independent of rapamycin or nutrient starvation, revealed by early M phase spindle structure emergence 15 min faster than WT cells. Hmt1S9A-expressing cells, in contrast, showed a 30 min delay in metaphase-anaphase spindle formation, independent of rapamycin treatment and similar to the rapamycin-induced delay in WT cells. Finally, maximal PI DNA staining intensities were observed at 90 min in all strains, confirming that both accelerated and delayed cell-cycle progression occur exclusively in early M phase, not in S phase.

Hmt1 Phosphorylation Is Required to Regulate *CLB2* mRNA Stability

Based on our observations thus far, we hypothesized that starvation and rapamycin promote *CLB2* mRNA decay through a mechanism requiring Hmt1 dephosphorylation and disassembly and loss of methyltransferase activity. This results in nuclear sequestering of Hmt1 methylation-dependent hnRNPs and a delay in cell-cycle progression into early M phase. Based on this hypothesis, we predicted that Hmt1S9E would be active, independent of rapamycin or starvation, promoting *CLB2* mRNA stability. In contrast, inactive Hmt1S9A would prevent *CLB2* mRNA accumulation in M phase. Therefore, as above, we counted *CLB2* nascent and cytoplasmic mRNAs by FISH in HMT1S9E and HMT1S9A mutant background strains as described previously (Zenklusen et al., 2008) (Figures 5H, 5I, S3D, and S3E). The nascent *CLB2* mRNA quantities peaked faster for HMT1S9E versus WT strain and accumulated on each *CLB2* allele within the first 50 min. However, cells expressing Hmt1S9A produced a broad *CLB2* mRNA wave peaking at 95 min and returning to basal levels at 155 min, independent of rapamycin or starvation.

Hmt1S9E strain exhibited elevated basal cytosolic *CLB2* mRNA throughout the cell cycle, with peaks of copy number similar to those observed in WT cells. Hmt1S9A strain, however, failed to accumulate *CLB2* mRNA throughout the cell cycle under all conditions. *ACT1* mRNA remained constant under all tested conditions and in all strains (Figure S3D).

Figure 5. Hmt1 Phosphorylation of Ser9 Is Essential and Required for Hmt1 Oligomerization, Methyltransferase Activity, and Resulting *CLB2* mRNA Accumulation and hnRNP Nuclear Export

(A) Flow chart of modified TAP tag purification for Hmt1 complexes with IgG precipitate AP treatments.

(B) TAP tag purification for Hmt1 complexes from Hmt1-expressing mutant strains. For each strain, cell lysates (lane Ly), last washes preceding TEV protease elution of TAP tag protein fusion (lane W), and IgG IPs (lane IP) were analyzed by immunoblotting.

(C) Methylation assays were performed with purified TAP-tagged proteins, fractionated on SDS-PAGE, and immunoblotted with anti-CBP (left panel). Npl3-TAP and Nab2-TAP were incubated with Hmt1WT-TAP (lane 1), Hmt1S9E-TAP (lane 2), or Hmt1S9A-TAP (lane 3) in the presence of [methyl-^{3}H]SAM, fractionated on SDS-PAGE, and detected by autoradiography (right panel).

(D) GFP intensities for hnRNPs in Hmt1WT- or Hmt1S9E-overexpressing background strains were quantified for 100 cells in rapamycin (200 nM) (in yellow). Cellular GFP signal was further segmented into nucleus (in blue), and cytoplasm (in red) was based on Nup49 nuclear membrane marker. Error bars, SD (n = 100).

(E–G) Hmt1 mutants in *cdc15-2* background strains grown at restrictive temperature were fixed, and the budded cell (E) and metaphase (F) and anaphase/telophase spindle proportions (G) were measured.

(H) Hmt1WT, Hmt1S9E, or Hmt1S9A mutant strains were synchronized, treated, stained with cy3.5 *CLB2* and cy5.0 *ACT1* mRNA probes mix (Figure S2A), imaged, and analyzed similarly to WT strain. Fluorescent nascent mRNA counting was performed for each time point. Error bars, SD (n = 50).

(I) Fluorescent mRNA counting was performed for each time point and distinct strain for cytosolic *CLB2* (left panel) and *ACT1* (right panel) mRNAs. Error bars, SD (n = 50).

(J) Fluorescent protein-tagged Clb2 quantification was performed for each *HMT1* mutant strain under similar conditions to the those of the WT strain. Error bars, SD (n = 100).

See also Figure S3.

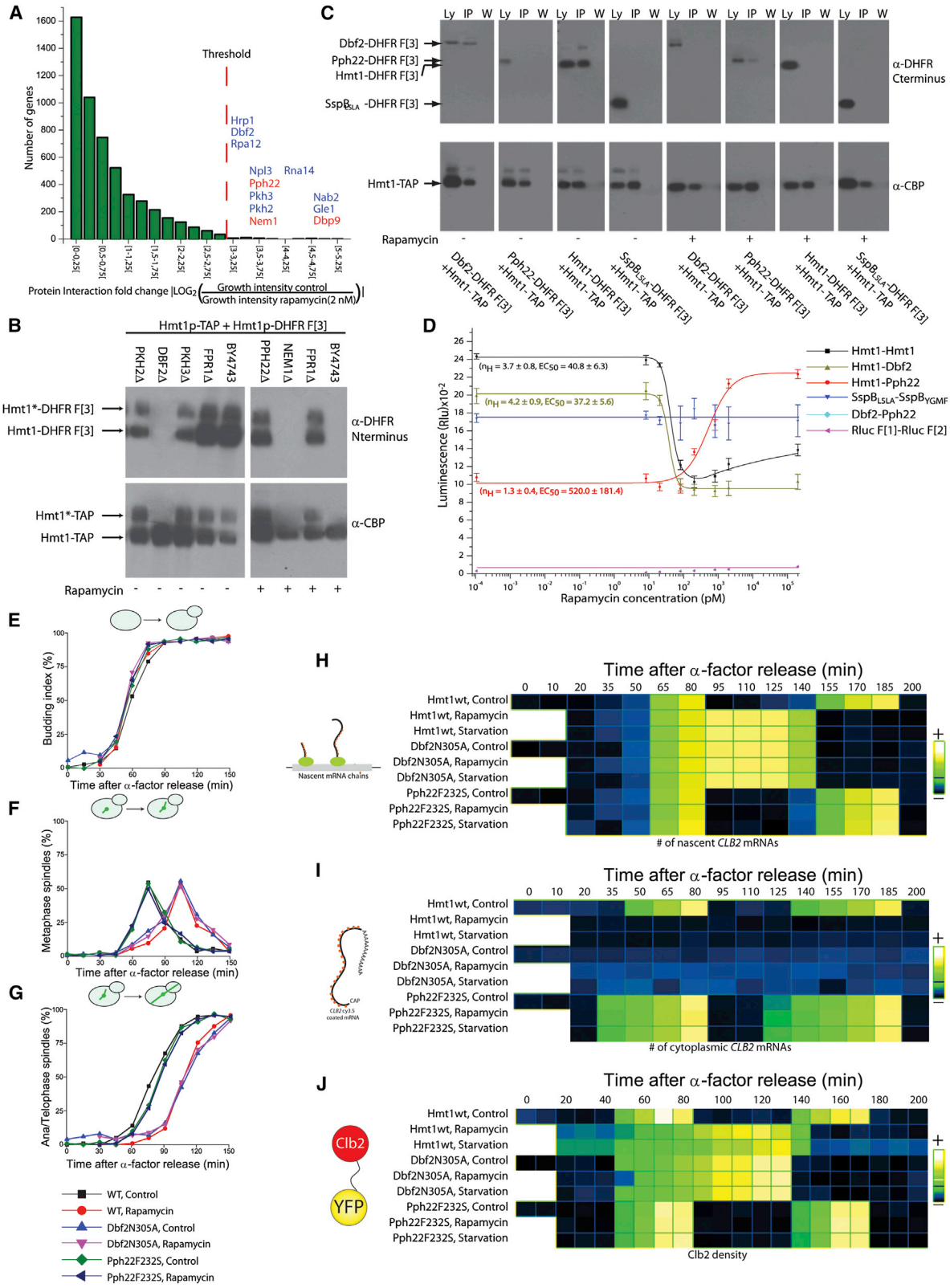

(legend on next page)

Hmt1 Phosphorylation Increases Clb2 Translation under Starvation and Rapamycin

Strains expressing Hmt1S9E or Hmt1S9A and Clb2-YFP were imaged and analyzed as described above (Figure 5J). Clb2 abundance was always elevated in the Hmt1S9E strain, except at 80 and 180 min when it was rapidly cleared from cells at mitotic exit. However, Hmt1S9A strain accumulated Clb2 slowly, 60 min after entering the cell cycle and over a 70 min period, reaching comparable numbers to control cells. It is thus clear that Hmt1 phosphorylation is required for both *CLB2* mRNA decay and Clb2 protein synthesis.

A Systematic Rapamycin-Dependent Hmt1 PPI Screen Identifies Potential Kinases and Phosphatases

We thus far determined that hnRNP localization and *CLB2* mRNA stability depend on Hmt1 phosphorylation. Next, we used the DHFR survival-selection protein-fragment complementation assay (PCA) to identify candidate kinases and phosphatases that interact with Hmt1 in a rapamycin-dependent manner (Pelletier et al., 1998). This assay was used to access the *S. cerevisiae* protein-protein interaction (PPI) network for approximately 92% of its proteins, in vivo and expressed at endogenous levels (Tarassov et al., 2008). We, performed the DHFR PCA screen between strains endogenously expressing Hmt1 fused to DHFR fragment F[1,2] and complementary fragment DHFR F[3] fused to a collection of 5,250 ORFs (Tarassov et al., 2008). Yeast strains were printed onto plates containing methotrexate DHFR PCA selective medium and sublethal rapamycin concentration (2 nM). Clones in which an interaction occurs between Hmt1 and another protein result in DHFR folding from the complementary fragments to which they are fused, resulting in reconstitution of methotrexate-resistant DHFR activity and thus cell growth and division. Colony-array images were analyzed to extract pixel intensity per colony in control and rapamycin-treated cells (Table S2). We calculated a fold-change in interaction for each tested Hmt1 pairwise interaction in rapamycin-treated versus control cells (Figure 6A). Thirty-four Hmt1 protein-protein interactions changed by at least 8-fold. These proteins were enriched in biological processes such as RNA 3′-end processing ($p < 10^{-6}$), posttranslational protein modification ($p < 10^{-4}$), and mRNA processing ($p < 10^{-3}$) (Table S2). Among these, the hnRNPs Nab2, Npl3, and Hrp1 showed reduced interaction with Hmt1 in rapamycin-treated reporter strains, along with several kinases, including Dbf2, Pkh2, and Pkh3. We also observed rapamycin-induced Hmt1 interaction with two phosphatases, Nem1 and Pph22, but not Pph22's paralog Pph21. We thus next tested whether Hmt1 is a substrate of these kinases and phosphatases.

Hmt1 Is a Substrate and Regulated by Dbf2 Kinase and Pph22 Phosphatase

We performed a genetic screen to determine whether any of the kinases or phosphatases described above could affect Hmt1 oligomerization. We generated Hmt1 dimerization reporter strains as above in *DBF2*Δ, *PKH2*Δ, *PKH3*Δ, *FPR1*Δ knockout strains under control condition and *NEM1*Δ, *PPH22*Δ, *FPR1*Δ backgrounds under rapamycin treatment and performed our IP assay (Figure 6B). The *FPR1*Δ strain was insensitive to rapamycin, serving as a control for TOR pathway activation (Heitman et al., 1991). We observed that Hmt1-TAP phosphorylation and Hmt1-DHFR F[3] coIP were abolished in the *DBF2*Δ strain but not in *PKH2*Δ, *PKH3*Δ and *FPR1*Δ strains. We repeated the experiments with the phosphatase candidates and found that, similar to the *FPR1*Δ strain, rapamycin-treated *PPH22*Δ strains retained Hmt1-TAP phosphorylation and Hmt1-DHFR F[3] coIP. These results suggest that Dbf2 and Pph22 are directly or indirectly essential for Hmt1 phosphorylation and dephosphorylation, respectively.

We verified the Dbf2 and Pph22 physical interactions by Hmt1-TAP IP. We generated strains as above to express Hmt1WT-TAP and DFHR F[3] fused to Dbf2, Pph22, Hmt1, and a protein from *H. influenzae*, $SspB_{LSLA}$, as negative control and performed our IP assay with extract from cells treated or not with rapamycin (200 nM) (Figure 6C). Hmt1-TAP coIP Dbf2-DHFR F[3] and Hmt1-DHFR F[3] under control conditions only, and Pph22-DHFR F[3] interacted weakly with Hmt1-TAP IPs only under rapamycin treatment. These results were specific for Hmt1, Dbf2, and Pph22 as $SspB_{LSLA}$-DHFR F[3] did not IP with Hmt1-TAP under both conditions. These results and those of the DHFR PCA suggest that both Pph22 and Dbf2 interact with Hmt1 in rapamycin and control conditions, respectively.

Figure 6. Dbf2 Kinase and Pph22 Phosphatase Differentially Regulate Hmt1 Phosphorylation State and *CLB2* Decay during Early M Phase in Rapamycin-Treated versus Control Cells

(A) Hmt1 DHFR PCA reporter strains for a collection of 5,250 ORFs were screened on solid-agar DHFR PCA-selective medium at sublethal rapamycin concentration (2 nM). Plates were photographed and analyzed, measuring pixel intensity over each colony. The protein-protein interaction fold-change distributions are displayed in a histogram. Strongest rapamycin-induced changes were displayed for both reduced (in blue) and increased (in red) interactions.

(B) Hmt1 dimerization reporter strains in *PKH2*Δ, *DBF2*Δ, *PKH3*Δ, and *FPR1*Δ and in *PPH22*Δ, *NEM1*Δ, and *FPR1*Δ treated with rapamycin for 6 hr were coIPed, and cell lysates were analyzed by immunoblotting.

(C) Hmt1-TAP and Dbf2, Pph22, or Hmt1 strains fused to DHFR F[3] or overexpressing a control $SspB_{LSLA}$-DHFR F[3] strain were treated with rapamycin for 6 hr. For each strain, cell lysates (lane Ly), IgG IPs (lane IP), and last wash (lane W) were analyzed by immunoblotting.

(D) Steady-state-level in vivo analysis of Hmt1, Dbf2, and Pph22 complexes with Hmt1 versus rapamycin reported by Rluc PCA. PPIs reported by Rluc PCA were tested for positive control $SspB_{LSLA}$-$SspB_{YGMF}$ interaction and negative control, noninteraction of Dbf2-Pph22 and Rluc PCA fragments expressed together. Error bars, SEM (n = 3).

(E–G) *cdc15-2* background strains expressing Pph22F232S or Dbf2N305A were fixed, and the budded cell proportions (E) and metaphase (F) and anaphase/telophase (G) spindle proportions were quantified.

(H and I) Pph22F232S- and Dbf2N305A-expressing strains were synchronized, treated, stained with a cy3.5 *CLB2*, *ACT1* mRNA probe mixture (Figure S3C), imaged, and analyzed similarly to the WT strain. Fluorescent nascent (H) and cytoplasmic (I) mRNA counting was performed for each strain. Error bars, SD (n = 50).

(J) Fluorescent-tagged Clb2 quantification was performed for Pph22F232S or Dbf2N305A mutant strains as done in WT strain. Error bars, SD (n = 100).

See also Figure S4 and Table S2.

To determine whether Dbf2 kinase could phosphorylate Hmt1 in vitro, we performed a kinase assay for yeast purified Hmt1WT, Hmt1S9E, and Hmt1S9A with radiolabeled [γ-^{32}P]-ATP in the presence of insect-cell-purified Dbf2-Mob1 or Dbf2N305A-Mob1 kinase-dead mutant (Mah et al., 2005) (Figure S4A). Hmt1WT was phosphorylated in vitro by Dbf2-Mob1. Absence of ^{32}P incorporation for the Dbf2N305-Mob1 kinase-dead mutant showed that phosphorylation was specific to Dbf2 and not to a copurified kinase from insect or yeast cells. In contrast, Hmt1S9E and Hmt1S9A did not incorporate ^{32}P in either kinase or kinase-dead samples, indicating that Hmt1 can be a direct Dbf2 substrate and that Ser9 is a unique Dbf2 phosphorylation site. The sequence around Ser9 is not a consensus for yeast Dbf2 (R-X-X-S) but is for human homologs (Hao et al., 2008).

Dbf2 Kinase Activity Is Necessary for Hmt1 Activation

To determine whether Dbf2 activity is required for Hmt1 methyltransferase activity, we performed the methylation assay as described above, incubating hnRNPs with purified yeast Hmt1-TAP from a Dbf2 kinase-dead mutant strain (Figure S4B). In the absence of Dbf2 kinase activity, Hmt1 did not methylate Npl3 or Nab2. These results confirm that Hmt1 requires phosphorylation by Dbf2 kinase for its activation.

Hmt1 Oligomerization and Dbf2 Binding to Hmt1 Are Ultrasensitive to Rapamycin, but Hmt1-Pph22 Binding Is Graded

We used the Rluc PCA to measure rapamycin dose responses of Hmt1-Hmt1, Dbf2-Hmt1, and Pph22-Hmt1 interactions in vivo. Hmt1-Dbf2 and Hmt1-Hmt1 complexes showed ultrasensitive dissociation to rapamycin (Hill coefficients of 4.2 $\pm$ 0.9 and 3.7 $\pm$ 0.8, respectively) and half-maximum effective concentrations (EC_{50}) of 37.2 pM and 40.8 pM (Figure 6D). In contrast, the Pph22-Hmt1 interaction was graded (Hill coefficient of 1.3 $\pm$ 0.4 and EC_{50} of 520.0 pM). These dynamics were specific as constitutive $SspB_{LSLA}$-$SspB_{YGMF}$ interaction was insensitive to rapamycin. Neither Dbf2-Pph22 nor PCA fragments interacted. Dbf2 and Pph22 protein abundances remained constant over the time course of these experiments, suggesting that observed rapamycin dose-response behavior was due to active processes, independent of protein concentration (Figure S4C).

Timing of M Phase Entry Depends on Dbf2 and Pph22 Activities

We tested whether Dbf2 and Pph22 competition for Hmt1 phosphorylation affects cell-cycle progression. We analyzed our cell-cycle markers in synchronized Dbf2 kinase-dead and Pph22 temperature-sensitive mutant strains and scored onset of budding (Figure 6E), DNA content (Figure S4D), and metaphase-to-telophase spindle formation (Figures 6F and 6G) (St-Pierre et al., 2009). We integrated catalytically dead DBF2N305A and temperature-sensitive PPH22F232S mutants directly into DBF2 and PPH22 loci, respectively, in *cdc15-2* background cells. We observed a 30 min delay in early M phase transition in the Dbf2N305A mutant strain, independent of growth conditions, revealed by metaphase-anaphase spindle emergence. Under all conditions, however, Pph22F232S-expressing cells displayed progression similar to that in WT vehicle-treated cells. The maximal PI DNA staining was observed after 90 min in all strains, suggesting that Dbf2 and Pph22 activities affect entry into M phase not exit from S phase.

Dbf2 Activity Increases and Pph22 Activity Decreases *CLB2* mRNA Stability

We predicted that loss of Dbf2 activity should increase and loss of Pph22 activity should decrease *CLB2* mRNA decay. As described previously for WT strains, we used FISH in strains endogenously expressing the Dbf2N305A or Pph22F232S mutants to count *CLB2* nascent and cytoplasmic transcripts in individual cells (Figures 6H, 6I, S4E, and S4F). We observed that the Dbf2N305A strain failed to accumulate *CLB2* transcripts, even under the control condition. However, the nascent *CLB2* transcripts continued to accumulate, showing that the mutant has no effect on *CLB2* transcription. In contrast, the Pph22F232S strain grown in rapamycin or starved accumulated nascent and cytoplasmic *CLB2* mRNA quantities comparable to the those of the WT strain in the control condition.

Dbf2 and Pph22 Activities Modulate Clb2 Protein Accumulation

We investigated whether the Dbf2 and Pph22 regulatory activities on Hmt1 modulate Clb2 protein levels. In DBF2N305A and PPH22F232S mutant strains expressing Clb2-YFP, we prepared, imaged, and analyzed fluorescence as described above for the WT strain (Figure 6J). The Dbf2N305A strain accumulated Clb2 slowly under all conditions, reaching a maximum at 130 min, before being cleared from the cell. In contrast, identical to conditions seen in control cells, the Pph22F232S strain showed persistent Clb2 levels under starvation and rapamycin.

DISCUSSION

We propose a general model by which normal cell-cycle progression or nutrient-dependent early M phase delay is mediated by phosphorylation-dependent Hmt1 oligomerization and activation (Figure 7A). We predict that during early M phase, Dbf2 phosphorylates Hmt1 and induces its ultrasensitive assembly and activation. Active Hmt1 methylates hnRNPs, which transport and stabilize *CLB2* transcripts. A feedback loop is propagated by *CLB2* mRNA being translated into B-cyclin, thus associating with Cdk1 to promote entry into mitosis. Increasing Dbf2 activity during early M phase further activates, in turn, Hmt1 (Hotz et al., 2012; Toyn and Johnston, 1994). Simultaneously, activated PP2A dephosphorylates Hmt1, leading to *CLB2* mRNA decay (Wang and Ng, 2006), leaving fewer transcripts available for B-cyclin translation. Given the cooperative Hmt1 activation by Dbf2, versus graded deactivation by Pph22, Dbf2 can activate Hmt1 if there is only a small decrease in Pph22 activity providing a means to tune cell-cycle progression.

Our results can explain how early M phase delay may occur in cells under rapamycin, starvation, or other stresses. It is known that Pph22 is released from the TAP42 complex when rapamycin-FKBP binds to TOR (Di Como and Arndt, 1996). In our model, Pph22 promotes the inactive monomerization of Hmt1, resulting in *CLB2* mRNA destabilization and, thus, delay of M phase entry. This basic circuit could be the target of multiple

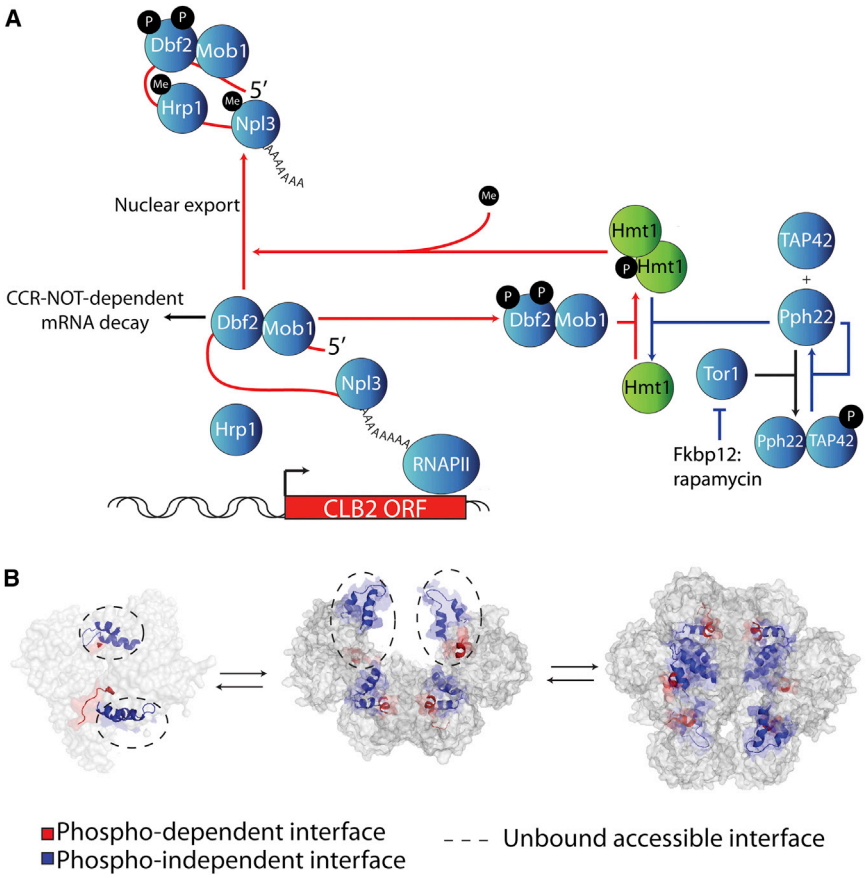

Figure 7. Hmt1 Oligomerization-Dependent Cell-Cycle Regulations

(A) Model of mechanism regulating *CLB2* mRNA decay during early M phase.

(B) Model of Hmt1 phosphorylation-dependent cooperative oligomerization.

stress-responsive kinases and phosphatases. Our genome-wide screen for Hmt1 revealed protein-protein interactions with alternative kinases and phosphatases, including the MAP kinases Pkh2 and Pkh3, which are implicated in cell-wall integrity (Roelants et al., 2002). These enzymes have been directly implicated in mRNA decay and inclusion in P bodies (Luo et al., 2011). Both of these phenomena may be mediated, at least in part, by concerted Pkh2 and Pkh3 association with Hmt1 and ribonucleoprotein complexes during their transport and stabilization. Furthermore, we observed an interaction with Nem1, a phosphatase implicated in nuclear membrane biogenesis and sporulation in yeast (Enyenihi and Saunders, 2003; Kim et al., 2007).

Our findings are consistent with evidence for Dbf2 roles in *CLB2* transcript decay during early M phase, the associations of Dbf2, Hmt1, and hnRNPs with gene loci, and their functions in nuclear export and mRNA stabilization in the cytoplasm (Trcek et al., 2011; Yu et al., 2004). In apparent contradiction to our results, Trcek et al. suggested that Dbf2 kinase activity is dispensable to *CLB2* transcript decay. We can resolve this discrepancy. Trcek et al. performed their experiments with a different Dbf2 "kinase-dead" mutant. It has, however, been reported that this mutant has residual kinase activity in vitro (Mah et al., 2005). We know that the Dbf2 activity during early M phase is minimal, not peaking until later in M phase (Hotz et al., 2012; Toyn and Johnston, 1994). We thus argue that the conclusions of Trcek et al. are correct in that Dbf2 does bind to the *CLB2* locus and regulates mRNA accumulation, but Dbf2 activity is not dispensable to mRNA-decay regulation by hnRNPs.

Hmt1 inactivation does not lead to the retention of *CLB2* mRNAs in the nucleus, but to an acute decay in the cytoplasm. Thus, methylation of hnRNPs does not primarily regulate *CLB2* mRNA nuclear export but rather primes the mRNA for regulation in the cytoplasm (e.g., decay). Consistent with these observations, two studies have shown that arginine methylation by Hmt1 acts as a signal for cotranscriptional assembly and hnRNP maturation (Chen et al., 2010; Yu et al., 2004). Nuclear priming of later mRNA-regulatory events by cotranscriptional hnRNP assembly is a common step prior to, for example, the deposition of the exon-exon junction complex for cytoplasmic mRNA quality control or assembly of hnRNPs for cytoplasmic mRNA localization (Shen et al., 2010). Presently, we do not know the protein composition of a *CLB2* hnRNP complex, but it is likely that its composition changes as a result of Hmt1 methylation. Consistent with our observation that different hnRNPs fail to accumulate in the cytoplasm when Hmt1 is inhibited, the lack of Nab2, Npl3, and Hrp1 methylation may prevent their binding to *CLB2* mRNA. Interestingly, a recent study showed that Hmt1p activity is required for Nab2 and Hrp1 binding to the CCR4-NOT complex (Kerr et al., 2011). If methylated Nab2 and Hrp1 are part of a stable, cytoplasmic *CLB2* messenger ribonucleoprotein particle (mRNP), this might suggest that interaction of CCR4-NOT with the *CLB2* mRNP is not sufficient to induce degradation, but that the complex is protected but "primed" for degradation. Degradation itself may require another signal.

In starved or rapamycin-treated cells, cytosolic mRNA no longer shows a cyclin increase in copy number, but the steady-state level remains constant, equal to that found in untreated cells. Thus, mRNA remains available for translation, and protein synthesis continues, albeit at a lower rate. An increase in Clb2-YFP levels without a change in *CLB2* mRNA levels could be caused by either an increase of the *CLB2* mRNA translation and/or an increase in Clb2 protein stability. Both scenarios are possible; however, as control of Clb2 protein stability is known to be regulated, this is the most likely mechanism (Seufert et al., 1995).

We demonstrated that Ser9 is required for Hmt1 phosphorylation and that oligomerization nucleates unphosphorylated

subunits, resulting in active hexameric Hmt1 complex (Figure 7B). Thus, only one of three subunits needs to be phosphorylated in order to induce dimers. Our results suggest that the phosphorylation-dependent dimerization interface allows phosphorylated Hmt1 to begin assembly into a dimer. The Hmt1 dimer subsequently assembles with nonphosphorylated subunits, resulting in a hexameric complex through a second, phosphorylation-independent interaction interface (Weiss et al., 2000).

Recent studies have demonstrated that the cell-cycle sharpness and coherence are regulated by transcriptional and biochemical feedback loops that can result in ultrasensitive and bistable transitions (Holt et al., 2008; Skotheim et al., 2008; Tsai et al., 2008). The model we describe is a positive feedback loop in which Dbf2 mediates cooperative Hmt1 assembly, and activation contributes to the early M phase control and exit from mitosis. The ultrasensitivity was evident in rapamycin-induced Dbf2 and Hmt1 disassembly in Hmt1 complexes. This regulatory design enables a tunable response to stresses that delay the cell cycle, while maintaining to a near constant the requirement for Clb2-Cdk1 complex activation to allow cell-cycle progression. The cooperative assembly and activation of Hmt1 adjust the rate of Clb2-Cdk1 activity by restraining *CLB2* mRNA availability. These predictions are consistent with the accelerated early M phase transitions in the constitutively active Hmt1S9E strain. The constitutively inactive Hmt1S9A mutant simply showed very low *CLB2* mRNA levels with slow Clb2 accumulation, resulting in early M phase delay. At the same time, the rapamycin dependence of the Pph22-Hmt1 complex is graded, suggesting that M phase is set to a critical threshold at which M phase will be delayed if the TOR pathway is downregulated by reduction of nutrients. Consistent with this argument, the Pph22 mutant resulted in recovery of a sharp change in *CLB2* mRNA accumulation in early M phase, independent of starvation or rapamycin.

Our results suggest that yeast have evolved a mechanism to adapt to a nutrient-limited environment by controlling mRNA stability. The cells thus benefit from an extended early M phase, allowing them to adapt to starvation by taking the time to synthesize the materials to generate viable daughter cells. We know that many RNAs, including ribosomal RNAs, other cyclins, and signaling-protein mRNAs, are under control of hnRNPs and thus Hmt1 activity (Barbet et al., 1996; Pestov and Shcherbik, 2012; Yu et al., 2004). Ribosomal RNA synthesis is a limiting factor in growth, and cyclins and signaling proteins regulate responses to stresses. It is thus possible that other kinases and phosphatases that act on Hmt1 respond to different signals, resulting in cell-cycle responses. Finally, Pph22 and Dbf2 are conserved from yeast to humans, and thus, it would be interesting to explore whether the same cell-cycle control mechanism is also conserved.

EXPERIMENTAL PROCEDURES

Strains, Plasmids, Growth Conditions, Buffers, and Primers

Tables S1 and S2 describe strains, plasmids, media, and buffers used in this study, their synchronization protocols, and growth conditions. Primers used to generate strains and diagnostic primers are listed in Table S4.

Single-Cell, Single-Molecule FISH

Table S4 describes FISH probes used in this study and the FISH procedures.

FACS Analysis of Strains Expressing GFP-Tagged Proteins

Table S3 describes the GFP strains used in this study and the FACS procedures.

FACS Analysis of Cell DNA Content

Table S3 describes the mutant strains used in this study for PI-stained DNA content analysis by FACS and the FACS procedures.

Fluorescent Protein Localization

Table S3 describes the GFP strains used in this study and the microscopy procedures.

Hmt1 DHFR PCA Large-Scale Screen

The DHFR screen procedures and strains were described previously (Tarassov et al., 2008). The Hmt1 differential protein interactions (rapamycin versus ethanol vehicle control) procedures are described in the Extended Experimental Procedures.

TAP-Tagged Protein IP

Table S3 describes the strains expressing TAP-tagged protein used in this study and the IP procedures.

Hmt1 Methyltransferase Assay

Methyltransferase activity assays are described in the Extended Experimental Procedures.

Rluc PCA Luminescence Detection

Table S3 describes the Rluc PCA strains used in this study. The Rluc PCA procedures were described previously (Malleshaiah et al., 2010). Details of the Hmt1 differential protein interactions (rapamycin versus ethanol vehicle control) are described in the Extended Experimental Procedures.

Purification of Dbf2-Mob1 Kinase Complex

Dbf2-FLAG was coIPed with Mob1 from Hi5 insect cells as described previously (Mah et al., 2005) and in the Extended Experimental Procedures.

Protein Kinase Assay

TAP-tagged Hmt1WT, Hmt1S9E, and Hmt1S9A, bound to 20 μl of beads representing ~100 ng of substrate protein, were dialyzed with DKB and incubated with Dbf2-Mob1 or Dbf2N305A-Mob1 (~13 ng of Dbf2 and 2 μCi [γ-^{32}P]-ATP) for 30 min at room temperature. Kinase reactions were stopped by addition of SDS-PAGE sample buffer, fractionated on SDS-PAGE, and detected by autoradiography.

SUPPLEMENTAL INFORMATION

Supplemental Information includes Extended Experimental Procedures, four figures, and four tables and can be found with this article online at http://dx.doi.org/10.1016/j.cell.2013.04.035.

ACKNOWLEDGMENTS

We thank Anne McBride for strains; Tatjana Trcek and Robert H. Singer (Albert Einstein College of Medicine) for *CBL2* and *ACT1* FISH probes, strains, and sharing data prior to publication; Raymond J. Deshaies and Tiffany K.J. Chang for providing us with Dbf2-expressing insect cell lines; Damien D'Amours for the gift of D754 strain and Tub1 immunostaining reagents; and Tatjana Trcek, Robert H. Singer, and Damien D'Amours for valuable discussions and comments. The authors acknowledge support from CIHR grants MOP-GMX-152556 and MOP-GMX- 231013 and NSERC of Canada grant 194582 (to S.W.M.) and CIHR grant MOP-BMB-232642 and the Canadian Foundation for Innovation (to D.Z.). D.Z. holds a FRSQ Chercheur Boursier Junior I.

Received: July 24, 2012
Revised: March 14, 2013
Accepted: April 4, 2013
Published: May 23, 2013

REFERENCES

Barbet, N.C., Schneider, U., Helliwell, S.B., Stansfield, I., Tuite, M.F., and Hall, M.N. (1996). TOR controls translation initiation and early G1 progression in yeast. Mol. Biol. Cell *7*, 25–42.

Blom, N., Gammeltoft, S., and Brunak, S. (1999). Sequence and structure-based prediction of eukaryotic protein phosphorylation sites. J. Mol. Biol. *294*, 1351–1362.

Chen, Y.C., Milliman, E.J., Goulet, I., Côté, J., Jackson, C.A., Vollbracht, J.A., and Yu, M.C. (2010). Protein arginine methylation facilitates cotranscriptional recruitment of pre-mRNA splicing factors. Mol. Cell. Biol. *30*, 5245–5256.

Chung, J., Kuo, C.J., Crabtree, G.R., and Blenis, J. (1992). Rapamycin-FKBP specifically blocks growth-dependent activation of and signaling by the 70 kd S6 protein kinases. Cell *69*, 1227–1236.

Di Como, C.J., and Arndt, K.T. (1996). Nutrients, via the Tor proteins, stimulate the association of Tap42 with type 2A phosphatases. Genes Dev. *10*, 1904–1916.

Enyenihi, A.H., and Saunders, W.S. (2003). Large-scale functional genomic analysis of sporulation and meiosis in Saccharomyces cerevisiae. Genetics *163*, 47–54.

Gandhi, S.J., Zenklusen, D., Lionnet, T., and Singer, R.H. (2011). Transcription of functionally related constitutive genes is not coordinated. Nat. Struct. Mol. Biol. *18*, 27–34.

Hao, Y., Chun, A., Cheung, K., Rashidi, B., and Yang, X. (2008). Tumor suppressor LATS1 is a negative regulator of oncogene YAP. J. Biol. Chem. *283*, 5496–5509.

Hector, R.E., Nykamp, K.R., Dheur, S., Anderson, J.T., Non, P.J., Urbinati, C.R., Wilson, S.M., Minvielle-Sebastia, L., and Swanson, M.S. (2002). Dual requirement for yeast hnRNP Nab2p in mRNA poly(A) tail length control and nuclear export. EMBO J. *21*, 1800–1810.

Heitman, J., Movva, N.R., and Hall, M.N. (1991). Targets for cell cycle arrest by the immunosuppressant rapamycin in yeast. Science *253*, 905–909.

Holt, L.J., Krutchinsky, A.N., and Morgan, D.O. (2008). Positive feedback sharpens the anaphase switch. Nature *454*, 353–357.

Hotz, M., Leisner, C., Chen, D., Manatschal, C., Wegleiter, T., Ouellet, J., Lindstrom, D., Gottschling, D.E., Vogel, J., and Barral, Y. (2012). Spindle pole bodies exploit the mitotic exit network in metaphase to drive their age-dependent segregation. Cell *148*, 958–972.

Houseley, J., and Tollervey, D. (2009). The many pathways of RNA degradation. Cell *136*, 763–776.

Kerr, S.C., Azzouz, N., Fuchs, S.M., Collart, M.A., Strahl, B.D., Corbett, A.H., and Laribee, R.N. (2011). The Ccr4-Not complex interacts with the mRNA export machinery. PLoS ONE *6*, e18302.

Kim, Y., Gentry, M.S., Harris, T.E., Wiley, S.E., Lawrence, J.C., Jr., and Dixon, J.E. (2007). A conserved phosphatase cascade that regulates nuclear membrane biogenesis. Proc. Natl. Acad. Sci. USA *104*, 6596–6601.

Lord, P.W., Selley, J.N., and Attwood, T.K. (2002). CINEMA-MX: a modular multiple alignment editor. Bioinformatics *18*, 1402–1403.

Luo, G., Costanzo, M., Boone, C., and Dickson, R.C. (2011). Nutrients and the Pkh1/2 and Pkc1 protein kinases control mRNA decay and P-body assembly in yeast. J. Biol. Chem. *286*, 8759–8770.

Mah, A.S., Elia, A.E., Devgan, G., Ptacek, J., Schutkowski, M., Snyder, M., Yaffe, M.B., and Deshaies, R.J. (2005). Substrate specificity analysis of protein kinase complex Dbf2-Mob1 by peptide library and proteome array screening. BMC Biochem. *6*, 22.

Malleshaiah, M.K., Shahrezaei, V., Swain, P.S., and Michnick, S.W. (2010). The scaffold protein Ste5 directly controls a switch-like mating decision in yeast. Nature *465*, 101–105.

McBride, A.E., Cook, J.T., Stemmler, E.A., Rutledge, K.L., McGrath, K.A., and Rubens, J.A. (2005). Arginine methylation of yeast mRNA-binding protein Npl3 directly affects its function, nuclear export, and intranuclear protein interactions. J. Biol. Chem. *280*, 30888–30898.

Nakashima, A., Maruki, Y., Imamura, Y., Kondo, C., Kawamata, T., Kawanishi, I., Takata, H., Matsuura, A., Lee, K.S., Kikkawa, U., et al. (2008). The yeast Tor signaling pathway is involved in G2/M transition via polo-kinase. PLoS ONE *3*, e2223.

Pelletier, J.N., Campbell-Valois, F.X., and Michnick, S.W. (1998). Oligomerization domain-directed reassembly of active dihydrofolate reductase from rationally designed fragments. Proc. Natl. Acad. Sci. USA *95*, 12141–12146.

Pestov, D.G., and Shcherbik, N. (2012). Rapid cytoplasmic turnover of yeast ribosomes in response to rapamycin inhibition of TOR. Mol. Cell. Biol. *32*, 2135–2144.

Pramila, T., Wu, W., Miles, S., Noble, W.S., and Breeden, L.L. (2006). The Forkhead transcription factor Hcm1 regulates chromosome segregation genes and fills the S-phase gap in the transcriptional circuitry of the cell cycle. Genes Dev. *20*, 2266–2278.

Roelants, F.M., Torrance, P.D., Bezman, N., and Thorner, J. (2002). Pkh1 and Pkh2 differentially phosphorylate and activate Ypk1 and Ykr2 and define protein kinase modules required for maintenance of cell wall integrity. Mol. Biol. Cell *13*, 3005–3028.

Romero-Santacreu, L., Moreno, J., Pérez-Ortín, J.E., and Alepuz, P. (2009). Specific and global regulation of mRNA stability during osmotic stress in Saccharomyces cerevisiae. RNA *15*, 1110–1120.

Seufert, W., Futcher, B., and Jentsch, S. (1995). Role of a ubiquitin-conjugating enzyme in degradation of S- and M-phase cyclins. Nature *373*, 78–81.

Shen, Z., St-Denis, A., and Chartrand, P. (2010). Cotranscriptional recruitment of She2p by RNA pol II elongation factor Spt4-Spt5/DSIF promotes mRNA localization to the yeast bud. Genes Dev. *24*, 1914–1926.

Skotheim, J.M., Di Talia, S., Siggia, E.D., and Cross, F.R. (2008). Positive feedback of G1 cyclins ensures coherent cell cycle entry. Nature *454*, 291–296.

St-Pierre, J., Douziech, M., Bazile, F., Pascariu, M., Bonneil, E., Sauvé, V., Ratsima, H., and D'Amours, D. (2009). Polo kinase regulates mitotic chromosome condensation by hyperactivation of condensin DNA supercoiling activity. Mol. Cell *34*, 416–426.

Tarassov, K., Messier, V., Landry, C.R., Radinovic, S., Serna Molina, M.M., Shames, I., Malitskaya, Y., Vogel, J., Bussey, H., and Michnick, S.W. (2008). An in vivo map of the yeast protein interactome. Science *320*, 1465–1470.

Toyn, J.H., and Johnston, L.H. (1994). The Dbf2 and Dbf20 protein kinases of budding yeast are activated after the metaphase to anaphase cell cycle transition. EMBO J. *13*, 1103–1113.

Trcek, T., Larson, D.R., Moldón, A., Query, C.C., and Singer, R.H. (2011). Single-molecule mRNA decay measurements reveal promoter- regulated mRNA stability in yeast. Cell *147*, 1484–1497.

Tsai, T.Y., Choi, Y.S., Ma, W., Pomerening, J.R., Tang, C., and Ferrell, J.E., Jr. (2008). Robust, tunable biological oscillations from interlinked positive and negative feedback loops. Science *321*, 126–129.

Wang, Y., and Ng, T.Y. (2006). Phosphatase 2A negatively regulates mitotic exit in Saccharomyces cerevisiae. Mol. Biol. Cell *17*, 80–89.

Weiss, V.H., McBride, A.E., Soriano, M.A., Filman, D.J., Silver, P.A., and Hogle, J.M. (2000). The structure and oligomerization of the yeast arginine methyltransferase, Hmt1. Nat. Struct. Biol. *7*, 1165–1171.

Yu, M.C., Bachand, F., McBride, A.E., Komili, S., Casolari, J.M., and Silver, P.A. (2004). Arginine methyltransferase affects interactions and recruitment of mRNA processing and export factors. Genes Dev. *18*, 2024–2035.

Zenklusen, D., Larson, D.R., and Singer, R.H. (2008). Single-RNA counting reveals alternative modes of gene expression in yeast. Nat. Struct. Mol. Biol. *15*, 1263–1271.